MULTIPOLE ANALYSIS

II.* GEOMAGNETIC SECULAR VARIATION

By R. W. James†

[*Manuscript received April* 18, 1969]

Summary

The method of multipole analysis described in Part I is applied to the Earth's magnetic field for various epochs between 1845 and 1965, allowing the geomagnetic secular variation to be illustrated by time trends in the multipole parameters. The rates of change of the multipole parameters are used to separate the secular variation into non-drifting, meridional drifting, and longitudinal drifting components, which are discussed in detail for the epoch 1965.

Introduction

This paper adopts the same notation and definitions as in Part I which, in brief, showed how to convert the spherical harmonic representation of an nth order potential

$$V_n = r^{-n-1} \sum_{m=0}^{n} (g_n^m \cos m\phi + h_n^m \sin m\phi) \mathrm{P}_n^m(\cos\theta), \tag{1}$$

into the multipole representation

$$V_n = (-)^n M_n \left(\prod_{i=1}^{n} (\boldsymbol{u}_{ni} . \nabla) \right) \frac{1}{r}. \tag{2}$$

The conversion from (1) to (2) entails finding the strength M_n and axes $\boldsymbol{u}_{ni}$ ($i = 1, \ldots, n$) from the Gaussian coefficients g_n^m and h_n^m ($m = 0, \ldots, n; h_n^0 = 0$).

Several authors (recently Winch and Slaucitajs 1966*a*, 1966*b*; Zolotov 1966; Winch 1967*a*, 1967*b*) have used the time trends in the multipole parameters M_n and $\boldsymbol{u}_{ni}$ to illustrate the secular variation (SV) of the Earth's magnetic field, and Winch (1968) has shown how to use the time derivatives $\dot{M}_n$ and $\dot{\boldsymbol{u}}_{ni}$ ($n = 1, 2$) to separate the dipole and quadrupole SV's into non-drifting, meridional drifting, and longitudinal drifting components. The method of Part I allows generalization of the above-mentioned ideas to any realistic order n, and in the present paper the geomagnetic fields for $n \leqslant 6$ are considered.

Rather than just accepting intuitively that the trends in M_n do actually depict the changing energy of the nth order field, a quantitative attempt is made to relate M_n to a more orthodox measure of strength, namely the r.m.s. field intensity on the Earth's surface $\bar{T}_n$. Some of the more intrinsic characteristics of Winch's separating

* Part I, *Aust. J. Phys.*, 1968, **21**, 455–64.

† Department of Applied Mathematics, University of Sydney, Sydney, N.S.W. 2006.

technique are demonstrated by a few simple examples, and the various components of SV are examined for the epoch 1965. Results for regions near Canada and Australia are considered separately and compared with world values.

Trends in Multipole Parameters

The changing patterns of the geomagnetic field are reflected in drifting multipole axes and decaying and growing multipole strengths. To determine the behaviour of the geomagnetic multipoles with time, data were considered for 13 different epochs between 1845 and 1965. Author references are shown in Table 1; journal references and a collation and discussion of the data have been given by McDonald and Gunst (1967). To reduce truncation errors (Vestine *et al.* 1963) only harmonic analyses of degree greater than four were included. The method of multipole analysis outlined in Part I was used to calculate the parameters M_n and $\boldsymbol{u}_{ni}$ ($i = 1, \ldots, n;\ n = 1, \ldots, 6$) for each epoch and, as a by-product (see Appendix), the derivatives $\dot{M}_n$ and $\dot{\boldsymbol{u}}_{ni}$ for epoch 1965.

Table 1

AUTHOR REFERENCES FOR 13 CHOSEN EPOCHS

Epoch	Author References	Order of Analysis	Epoch	Author References	Order of Analysis
1845	Adams (1900)‡	6	1955	Finch and Leaton (1957)‡	6
1882·5*	Adams (1900)‡	6		Jensen and Whitaker (1960)‡	7
	Fritsche (1897)‡	7		Kautzleben (1965*b*)‡	> 6
1905†	McDonald and Gunst (1967)	6		Vestine *et al.* (1963*a*;	
1915†	McDonald and Gunst (1967)	6		2 analyses)‡	12
1922	Dyson and Furner (1923)‡	> 4	1958	Adam *et al.* (1962)‡	6
1925†	McDonald and Gunst (1967)	6		Nagata and Oguti (1962)‡	6
1935†	McDonald and Gunst (1967)	6	1960	Adam *et al.* (1964)‡	6
1942	Jones and Melotte (1953)‡	6		Cain *et al.* (1965)‡	7
1945	Fanselau *et al.* (1964)	15		Fougere (1965)	> 7
	Vestine *et al.* (1947*b*)‡	6		Jensen and Cain (1962)‡	6
1955	Adam *et al.* (1962;		1965	Hurwitz *et al.* (1966)‡	12
	3 analyses)‡	6		Leaton *et al.* (1965)‡	8

* The data for this epoch were obtained by averaging the 1880 data of Adams (1900)‡ and the 1885 data of Fritsche (1897)‡.

† The data for these epochs were calculated by McDonald and Gunst (1967) by linearly extrapolating the data of Vestine *et al.* (1947*b*)‡.

‡ These references may be found in the bibliography of McDonald and Gunst (1967).

For each of the six fields ($n = 1, \ldots, 6$) a map was drawn showing (1) the pole positions (θ_{ni}, ϕ_{ni}) of the axes $\boldsymbol{u}_{ni}$ for the 13 chosen epochs, (2) the tangential velocities $\dot{\boldsymbol{u}}_{ni}$ derived from the 1965 main field and SV coefficients of Leaton, Malin, and Evans (1965; hereafter referred to as LME), and (3) the isolines of the 1965 LME vertical intensity Z. The following brief summary of the pole motions is derived from these maps and Table 2, which lists the results of a multipole analysis of the 1965 LME data:

(1) The geomagnetic dipole axis has remained almost stationary. In 1965 the pole was at $\theta = 168\cdot5°, \phi = 109\cdot7°$ and drifting slowly westward at about $0\cdot07$ deg yr^{-1}.

(2) Apart from one almost stationary octupole axis, the quadrupole ($n = 2$) and octupole ($n = 3$) axes have undergone significant drifts to the west and in 1965 continued to drift westward with angular velocities averaging more than $0\cdot3$ deg yr^{-1}.

In 1965, one quadrupole axis had a large meridional drift of about 0·2 deg yr^{-1} and one octupole axis had a meridional drift of about 0·1 deg yr^{-1}.

(3) In 1965 all fourth-order poles were just to the east of their 1845 positions but were heading west with only one showing noticeable meridional drift ($\sim$ 0·07 deg yr^{-1}). However, the pole positions for the various epochs indicate that two of the fourth-order poles have undergone significant meridional drifts during the 120 year period considered.

(4) The fifth- and sixth-order fields are the only ones to exhibit very large meridional drifts (0·1–0·5 deg yr^{-1}) although large east and west drifts are also present. The poles have generally moved more rapidly and more erratically than the lower order poles but uncertainties in the higher order data are undoubtedly a source of some apparent motion.

(5) Apart from one third-order pole, one fifth-order pole, and three sixth-order poles, all vectors $\dot{\boldsymbol{u}}_{ni}$ had westward rather than eastward components in 1965.

Table 2

RESULTS OF MULTIPOLE ANALYSIS OF 1965 LME DATA

Multipole strengths $n!M_n$, pole coordinates (θ_{ni}, ϕ_{ni}), rates of change $n!\dot{M}_n$ and $(\dot{\theta}_{ni}, \dot{\phi}_{ni})$, and best-fit westward drifts U_n are shown. Here a = 1 Earth radius

n	$n!M_n$ (γa^{n+2})	$n!\dot{M}_n$ (γa^{n+2} yr^{-1})	θ_{ni} (deg)	$\dot{\theta}_{ni}$ (deg yr^{-1})	ϕ_{ni} (deg)	$\dot{\phi}_{ni}$ (deg yr^{-1})	$-U_n$ (deg yr^{-1})
1	30987	−15·6	168·5	0·00	109·7	−0·07	−0·07
2	4864	16·9	23·0	−0·06	31·6	−0·55	−0·24
			104·9	0·21	331·9	−0·11	
3	4135	4·9	20·7	0·02	344·5	−0·40	−0·09
			58·0	−0·02	141·4	0·05	
			63·4	−0·10	223·8	−0·20	
4	2609	0·35	24·4	0·00	109·3	−0·22	−0·09
			35·8	−0·02	216·9	−0·29	
			56·7	−0·07	308·0	−0·07	
			68·0	0·02	42·4	−0·07	
5	1052	2·6	16·3	−0·15	278·1	−0·49	−0·03
			39·3	−0·20	340·3	−0·25	
			47·2	−0·11	188·7	−0·27	
			64·9	0·35	53·7	−0·13	
			90·5	−0·20	353·7	0·11	
6	973	−0·0011	30·9	0·15	240·8	−0·04	−0·07
			34·5	0·19	4·4	0·26	
			42·3	0·54	132·0	0·17	
			76·6	−0·12	49·6	−0·19	
			80·8	−0·18	118·9	−0·33	
			95·4	0·35	356·6	0·18	

Enhanced by the dominance (see Part I and Table 2) of the quadrupole and octupole fields amongst the non-dipole fields, the principal characteristic to be inferred from the above summary is the tendency for westward drift. This is a well-established property of the Earth's field and the subject of many investigations. Several recent attempts to estimate a rate of drift have been published (Bullard *et al.* 1950; Whitham 1958; Yukutake 1962), but a simple way of obtaining the drift U_n of an nth order field is to use the equation (Nagata 1962, 1965; see also James 1968)

$$U_n = \left(\sum_{m=0}^{n} m(\dot{g}_n^m h_n^m - \dot{h}_n^m g_n^m)\right) \div \left(\sum_{m=0}^{n} m^2\{(g_n^m)^2 + (h_n^m)^2\}\right). \tag{3}$$

The SV coefficients caused by a uniform westward drift (WD) U_n are

$$\dot{g}_n^m(WD) = mU_n h_n^m \qquad \text{and} \qquad \dot{h}_n^m(WD) = -mU_n g_n^m,$$

and the criterion used to derive (3) is minimization of the r.m.s. difference between the field defined by $\dot{g}_n^m(WD)$ and $\dot{h}_n^m(WD)$ and the observed SV field with coefficients $\dot{g}_n^m$ and $\dot{h}_n^m$.

Table 2 lists meridional drifts $\dot{\theta}_{ni}$ and longitudinal drifts $\dot{\phi}_{ni}$, calculated from $\boldsymbol{u}_{ni}$ and $\dot{\boldsymbol{u}}_{ni}$, for the 1965 LME data, and includes for comparison the corresponding rates U_n from (3). The estimate U_n is accurate only when the drift is almost purely longitudinal and uniform (in space). The scatter of the values of $\dot{\phi}_{ni}$ and the existence of significant meridional drifts $\dot{\theta}_{ni}$ shows that the geomagnetic field does not drift according to such a simple model. However, there is a definite tendency for westward drift, emphasized by the negative signs in the last two columns of Table 2.

Figure 1 illustrates the variation in time of the field strengths M_n ($n = 1, \ldots, 6$). The curves are not best fits but are merely intended to show the general trends derived from the 13 epochs. In brief summary we note:

(1) The dipole strength M_1 has decreased continuously at an average rate of about $15 \cdot 3\ \gamma a^3\,\mathrm{yr}^{-1}$, where a is the Earth's radius. The 1965 rate of decrease from the LME data was $15 \cdot 6\ \gamma a^3\,\mathrm{yr}^{-1}$. The M_1 curve in Figure 1 suggests that the rate of decrease just after the turn of the century was somewhat larger than the 1965 or average value, and closer examination of the smaller-scale variations of M_1 has tempted some observers (Bullard 1953; Macht 1954) to infer that a minimum in M_1 occurred between 1930 and 1952. However, the overall trend implied by the curve in Figure 1 is for a continued decrease in strength. Indeed, by studying a more consistent set of data, Leaton and Malin (1967) have concluded that in the period $1942 \cdot 5$ to $1962 \cdot 5$ the rate of decrease of M_1 began to increase; low altitude satellite observations (Cain and Langel 1968) suggest that the increasing rate of decrease persisted in 1967.

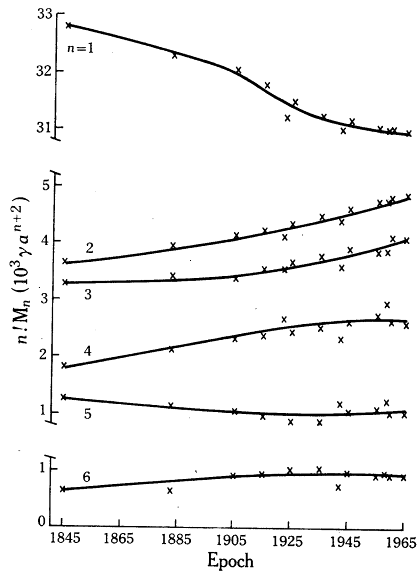

Fig. 1.—Secular trends in geomagnetic multipole strengths.

(2) The fifth- and sixth-order strengths have changed little during the 120 year period considered, but the other non-dipole strengths have all increased, reflecting a growing complexity of the total field.

It is generally accepted that M_n may legitimately be called the strength of the field since for given $\boldsymbol{u}_{ni}$ $(i = 1, \ldots, n)$ the field geometry (as determined by the isolines) is fixed and M_n determines the intensity. Just how reliably the trends in M_n do reflect changes in the more usual strength parameters like r.m.s. intensity or magnetostatic energy has not been previously investigated. It was therefore decided to look more closely at the dimensionless ratio $\rho_n = a^{n+2}\bar{T}_n(n!M_n)^{-1}$ and at the possible range of values that this function (of the $\boldsymbol{u}_{ni}$) may take. Using the relation (derived in Part I)

$$\bar{T}_n = \left((n+1) \sum_{m=0}^{n} \{(g_n^m)^2 + (h_n^m)^2\}\right)^{\frac{1}{2}} a^{-(n+2)}$$

and substituting from equations (5) and (6) of Part I, it is found that

$$\rho_1 = \sqrt{2}, \qquad \rho_2 = \tfrac{3}{2}\{1+\tfrac{1}{3}(\boldsymbol{u}_{21}\cdot\boldsymbol{u}_{22})^2\}^{\frac{1}{2}}. \tag{4}$$

So ρ_1 is independent of $\boldsymbol{u}_{11}$ and ρ_2 is only weakly dependent on the choice of $\boldsymbol{u}_{21}$ and $\boldsymbol{u}_{22}$ (from (4) we have $1\cdot5 \leqslant \rho_2 \leqslant \sqrt{3}$). For $n > 2$ it is difficult to give theoretical values for the range of ρ_n, but for the case where all the $\boldsymbol{u}_{ni}$ coincide, say with the z axis, Rodrigue's formula

$$\left(-\frac{\partial}{\partial z}\right)^n \frac{1}{r} = n!\,\mathrm{P}_n^0(\cos\theta)\,r^{-(n+1)}$$

indicates that ρ_n can take values as large as $(n+1)^{\frac{1}{2}}$. To obtain some idea of the minimum of ρ_n and of the sensitivity to the choice of vectors $\boldsymbol{u}_{ni}$, a uniformly distributed random-number generator was used to produce, for each order n, 1000 sets of unit vectors $\boldsymbol{u}_{ni}$ $(i = 1, \ldots, n)$. The Gaussian coefficients corresponding to each set were calculated through relations (6) of Part I and ρ_n was then found using the formula for $\bar{T}_n$. The results in Table 3 indicate that whilst sensitivity increases with n, ρ_n is, for $1 \leqslant n \leqslant 6$, only a very weak function of the $\boldsymbol{u}_{ni}$. Now the geomagnetic multipole axes have varied "slowly" as opposed to randomly during the period 1845–1965. Thus low sensitivity would suggest that the geomagnetic ρ_n values should have remained approximately constant during this time — a prediction verified by the results in Table 4. Comparison of Tables 3 and 4 shows that for the Earth's field the ratios ρ_n are near the lower end of the spectrum of numbers suggested by the random number search. In particular, ρ_2 has been almost exactly constant in time at $1\cdot500$, which, as seen from the equation for ρ_2 in (4) results from the near perpendicularity of the quadrupole axes (in 1965 $\boldsymbol{u}_{21}\cdot\boldsymbol{u}_{22} \approx -0\cdot05$). It is concluded that for the geomagnetic fields $n!M_n a^{-(n+2)}$ can be regarded as approximately proportional to $\bar{T}_n$ (which in turn is proportional (see Part I) to the r.m.s. vertical intensity $\bar{Z}_n$ and the r.m.s. horizontal intensity $\bar{H}_n$). Moreover, the constant of proportionality ρ_n is in the range $0\cdot8$–$1\cdot5$ for all the geomagnetic multipoles considered. The curves in Figure 1 then do accurately reflect the trends in intensity and thus energy of the fields. From the above discussion it seems that it would be desirable to modify the definition of multipole strength. A strength defined by $M'_n = n!M_n a^{-(n+2)}$ would have several advantages. Firstly, the inclusion of the factor a^{n+2} would allow M'_n to have units of magnetic force, more in line with the title "strength". Secondly, the inclusion of the scale factor $n!$ would make M'_n comparable in magnitude with the r.m.s. field intensity on the Earth's surface; other authors have included $n!$ on mathematical grounds (Maxwell 1892; Zolotov 1966).

Table 3

RANGE OF VALUES TAKEN BY $\rho_n = a^{n+2}\overline{T}_n(n!M_n)^{-1}$ AS DETERMINED BY RANDOM NUMBER SEARCH

The theoretical maximum of ρ_n is $(n+1)^{\frac{1}{2}}$

n	ρ_n	$(n+1)^{\frac{1}{2}}$	n	ρ_n	$(n+1)^{\frac{1}{2}}$
1	1·41–1·41	1·41	4	1·16–2·14	2·24
2	1·50–1·73	1·73	5	1·02–2·07	2·45
3	1·30–1·97	2·00	6	0·83–2·16	2·64

Table 4

RATIOS $\rho_n = a^{n+2}\overline{T}_n(n!M_n)^{-1}$ FOR GEOMAGNETIC FIELD AT 13 CHOSEN EPOCHS

Epoch	$n = 1$	2	3	4	5	6
1845	1·4142	1·500	1·377	1·34	1·17	1·0
1882·5	1·4142	1·501	1·375	1·33	1·19	1·1
1905	1·4142	1·501	1·350	1·29	1·26	0·9
1915	1·4142	1·500	1·339	1·27	1·26	0·9
1922	1·4142	1·505	1·363	1·35	—	—
1925	1·4142	1·501	1·338	1·27	1·31	0·9
1935	1·4142	1·500	1·341	1·26	1·32	0·9
1942	1·4142	1·501	1·335	1·32	1·19	1·1
1945	1·4142	1·500	1·345	1·27	1·22	0·9
1955	1·4142	1·500	1·373	1·24	1·17	0·9
1958	1·4142	1·500	1·357	1·24	1·10	0·9
1960	1·4142	1·500	1·375	1·27	1·31	0·8
1965	1·4142	1·501	1·371	1·25	1·31	0·9

The forms of the curves in Figure 1 raise the possibility of energy balance between the dipole and non-dipole fields. To investigate this question one should not only consider the energy of the field outside the Earth but also the interior energy which actually makes up most of the total energy. Calculations of interior energy require inward extrapolation of the field resulting in amplification of the relative contributions to the energy from the less accurately known higher order harmonics, and thus inescapably contain large errors. However, it may be definitely stated that there has been a significant decrease in the external magnetostatic energy

$$E = \tfrac{1}{2}a^3 \sum_{n=1}^{6} \overline{T}_n^2 (2n+1)^{-1}. \qquad (5)$$

The average rate of decrease of E during the period 1845–1965 was about 8% per century. The same rate is obtained independently by substituting the LME 1965 data into

$$\frac{\mathrm{d}E}{\mathrm{d}t} = \sum_{n=1}^{6}\left(\frac{n+1}{2n+1}\right)a^{-2n-1}\sum_{m=0}^{n}(g_n^m\,\dot{g}_n^m + h_n^m\,\dot{h}_n^m),$$

obtained by differentiating (5).

Separation of SV into Drifting and Non-drifting Components

The SV of the nth order geomagnetic potential V_n is usually represented by Gaussian coefficients $\dot{g}_n^m$ and $\dot{h}_n^m$ in the same way that g_n^m and h_n^m describe V_n in (1). The time derivatives of the multipole parameters allow an alternative representation. Following Winch (1968), differentiate (2) to obtain

$$SV = ND+D, \tag{6}$$

where

$$ND = (-)^n\dot{M}_n\left(\prod_{i=1}^{n}(\boldsymbol{u}_{ni}\cdot\nabla)\right)\frac{1}{r} \tag{7}$$

and

$$D = (-)^n M_n\left(\sum_{i=1}^{n}(\dot{\boldsymbol{u}}_{ni}\cdot\nabla)\prod_{\substack{j=1\\ j\neq i}}^{n}(\boldsymbol{u}_{nj}\cdot\nabla)\right)\frac{1}{r}. \tag{8}$$

By comparing (7) with equations (1) and (2), the Gaussian coefficients of ND are seen to be

$$\dot{g}_n^m(ND) = \dot{M}_n g_n^m/M_n, \qquad \dot{h}_n^m(ND) = \dot{M}_n h_n^m/M_n. \tag{9}$$

Hence from (6), the Gaussian coefficients of D are

$$\dot{g}_n^m(D) = \dot{g}_n^m - \dot{M}_n g_n^m/M_n, \qquad \dot{h}_n^m(D) = \dot{h}_n^m - \dot{M}_n h_n^m/M_n.$$

Since the drifts $\dot{\boldsymbol{u}}_{ni}$ of the axes do not contribute to ND, Winch has called ND the non-drifting component of SV; similarly, since only the drifts $\dot{\boldsymbol{u}}_{ni}$ are sources of D, D was termed the drifting component. Because the $\dot{\boldsymbol{u}}_{ni}$ are tangential to the Earth's surface, D is associated with rotational characteristics of SV rather than with changes in field strength or radial characteristics which must be reflected in ND. It is interesting to consider a few simple examples that illustrate more explicitly the character of Winch's separation technique:

(i) *Non-drifting fields.* Consider a potential whose geometrical structure is unchanging in time but whose intensity varies. Multipole analysis would reveal a superposition of multipoles with stationary axes and time varying strengths. Moreover, if the shape of the field is to be preserved, the SV (in this case purely ND) coefficients $\dot{g}_n^m$ and $\dot{h}_n^m$ must be proportional to the main field coefficients g_n^m and h_n^m. It follows from (9) that $\dot{M}_n/M_n$ would be independent of n. If $\dot{M}_n/M_n$ were different for different n's, the relative contributions to the overall field structure from the various multipoles would change in time, and hence the field, although still non-drifting, would change shape. In both the above cases, equation (3) would also regard the fields as having no drift.

(ii) *Uniformly drifting fields.* Consider a field rotating in rigid-body manner about some axis so that any observer rotating in the same way measures no change in the field characteristics. Multipole analysis would yield a superposition of multipoles with constant strengths and axes all rotating at the same rate about the same axis. Equation (3) would only yield the correct value of the angular speed if the spherical harmonic coefficients used in (3) were referred to the rotation axis as polar axis.

(iii) *Moving internal source.* Consider an nth order multipole source defined by $M_n, \boldsymbol{u}_{ni}$ $(i = 1, \ldots, n)$ situated at the point $\boldsymbol{R}$ and with velocity $\dot{\boldsymbol{R}}$. The potential in the region $r > R$ due to this source can be shown (James 1969, equations (31) and (36)) to be

$$V = \sum_{k=n}^{\infty} V_k,$$

where

$$V_k = \frac{(-)^n M_n}{(k-n)!}\left((\boldsymbol{R}.\nabla)^{k-n}(\boldsymbol{u}_{n1}.\nabla)\ldots(\boldsymbol{u}_{nn}.\nabla)\right)\frac{1}{r}. \tag{10}$$

So multipole analysis would yield a superposition of multipoles with orders greater than and equal to n, with the kth order multipole having strength $M_n R^{k-n}/(k-n)!$ and axes $\boldsymbol{u}_{ki}$ $(i = 1, \ldots, k)$ given by

$$\begin{aligned} \boldsymbol{u}_{ki} &= \boldsymbol{u}_{ni}, \qquad && i \leqslant n, \\ &= \boldsymbol{R}/R, && i > n. \end{aligned}$$

The SV of this field due to the motion of the source can be separated into ND and D components by differentiating (10). We obtain:

(1) an ND component based on a rate of change of strength,

$$M_n R^{k-n-1}\dot{R}/(k-n-1)!,$$

proportional to the radial speed of the source; and

(2) a D component caused by the axes $\boldsymbol{u}_{ki}$ $(i > n)$ drifting with the angular velocity $\mathrm{d}(\boldsymbol{R}/R)/\mathrm{d}t$ of the source.

The n stationary axes $\boldsymbol{u}_{ki}$ $(i \leqslant n)$ represent the geometry of the field about the source as origin, whilst the axes $\boldsymbol{u}_{ni}$ $(i > n)$ rotate so that they always point in the direction of the source.

Example (iii) above emphasizes the intrinsic rotational versus non-rotational character of Winch's method of defining D and ND.

The drifting field D, given by (8), may be separated into contributions from the meridional and longitudinal drifts of the axes. To do this, we note that

$$\dot{\boldsymbol{u}}_{ni} = \dot{\theta}_{ni}\boldsymbol{\mu}_{ni} + \dot{\phi}_{ni}\boldsymbol{\lambda}_{ni},$$

where, with $\boldsymbol{u}_{ni} = (u_{ni}, v_{ni}, w_{ni})$ as in Part I,

$$\boldsymbol{\mu}_{ni} = (u_{ni}w_{ni}, v_{ni}w_{ni}, w_{ni}^2 - 1)(1 - w_{ni}^2)^{-\frac{1}{2}}$$

and

$$\boldsymbol{\lambda}_{ni} = (-v_{ni}, u_{ni}, 0).$$

TABLE 5

SPHERICAL HARMONIC COEFFICIENTS FOR 1965 LME SECULAR VARIATION AND COMPONENT FIELDS

Units are $\gamma a^{n+2}\,\mathrm{yr}^{-1}$ where a = 1 Earth radius

n	m		*SV*	*ND*	*D*	*MD*	*LD*	*WD*
1	0	g	15·5	15·3	0·2	0·2	0·0	0·0
	1	g	8·3	1·0	7·3	−0·3	7·5	7·5
		h	0·6	−2·9	3·5	0·8	2·7	2·7
2	0	g	−26·6	−5·6	−21·0	−14·9	−6·0	0·0
	1	g	−1·3	10·2	−11·5	−6·0	−5·5	−8·2
		h	−11·4	−6·9	−4·5	−1·6	−2·9	−12·2
	2	g	1·3	5·5	−4·2	−5·3	1·1	0·8
		h	−18·2	0·3	−18·5	−0·3	−18·2	−13·1
3	0	g	0·0	1·4	−1·4	5·0	−6·4	0·0
	1	g	−9·5	−2·4	−7·1	−1·0	−6·1	−0·7
		h	3·2	−0·5	3·7	2·6	1·1	3·1
	2	g	−1·9	1·5	−3·4	−3·4	0·0	0·8
		h	1·6	0·3	1·3	0·9	0·4	−4·0
	3	g	−0·6	1·0	−1·6	−0·1	−1·5	−0·7
		h	−8·5	−0·2	−8·3	0·0	−8·3	−4·0
4	0	g	0·6	0·1	0·5	0·6	−0·1	0·0
	1	g	1·0	0·1	0·9	0·6	0·3	0·3
		h	3·0	0·0	3·0	2·0	1·0	−1·3
	2	g	−2·2	0·1	−2·3	−0·6	−1·7	−0·9
		h	−0·7	0·0	−0·7	−0·6	−0·1	−1·6
	3	g	0·2	−0·1	0·3	0·8	−0·5	0·1
		h	2·7	0·0	2·7	0·4	2·3	1·9
	4	g	−3·0	0·0	−3·0	−0·3	−2·8	−1·6
		h	−2·7	0·0	−2·7	0·3	−2·9	−1·7
5	0	g	0·8	−0·4	1·2	1·1	0·1	0·0
	1	g	0·4	0·9	−0·5	−1·4	0·9	0·0
		h	1·9	0·0	1·9	1·2	0·7	−0·2
	2	g	1·6	0·6	1·0	1·2	−0·2	0·1
		h	2·3	0·3	2·0	2·6	−0·6	−0·3
	3	g	−0·3	0·0	−0·3	0·6	−0·9	−0·2
		h	−1·8	−0·3	−1·5	−1·5	−0·1	0·0
	4	g	−1·1	−0·4	−0·7	0·1	−0·8	−0·2
		h	1·4	−0·2	1·6	−0·1	1·8	0·4
	5	g	1·7	−0·2	1·9	0·7	1·1	0·2
		h	0·5	0·2	0·3	−0·8	1·1	0·2
6	0	g	0·0	0·0	0·0	0·8	−0·8	0·0
	1	g	−0·5	0·0	−0·5	0·2	−0·7	0·0
		h	−2·2	0·0	−2·2	−0·5	−1·7	−0·1
	2	g	1·8	0·0	1·8	1·7	0·1	0·2
		h	0·2	0·0	0·2	0·3	−0·1	0·0
	3	g	1·4	0·0	1·4	1·1	0·3	0·2
		h	0·9	0·0	0·9	−0·3	1·2	0·9
	4	g	0·6	0·0	0·6	0·3	0·3	−0·2
		h	−2·1	0·0	−2·1	−1·2	−0·9	−0·1
	5	g	0·2	0·0	0·2	0·0	0·2	−0·1
		h	−0·1	0·0	−0·1	−0·4	0·3	−0·1
	6	g	−2·2	0·0	−2·2	−2·2	0·0	0·0
		h	−0·2	0·0	−0·2	−0·1	−0·1	0·9

The meridional drifting component of D is then

$$MD = (-)^n M_n \left(\sum_{i=1}^{n} \dot{\theta}_{ni}(\boldsymbol{\mu}_{ni}\cdot\nabla) \prod_{\substack{j=1\\ j\neq i}}^{n} (\boldsymbol{u}_{nj}\cdot\nabla) \right) \frac{1}{r}$$

and the longitudinal drifting component is

$$LD = (-)^n M_n \left(\sum_{i=1}^{n} \dot{\phi}_{ni}(\boldsymbol{\lambda}_{ni}\cdot\nabla) \prod_{\substack{j=1\\ j\neq i}}^{n} (\boldsymbol{u}_{nj}\cdot\nabla) \right) \frac{1}{r}.$$

The Gaussian coefficients $\dot{g}_n^m(MD)$, $\dot{h}_n^m(MD)$, $\dot{g}_n^m(LD)$, and $\dot{h}_n^m(LD)$ can be calculated from the recurrence relations (6) of Part I, and are listed for the LME data in Table 5 together with the coefficients of SV, ND, D, and WD, the last being included for comparison with the LD coefficients. Even allowing for the fact that westward drift cannot create zonal ($m = 0$) SV coefficients, there does not appear to be any obvious connection between the individual WD and LD coefficients apart from the special dipole case. Yet the isoline map of the LD $\dot{Z}$ field (Fig. 2(*d*)) is very similar to the isoline map (not shown) obtained by superimposing the WD $\dot{Z}$ field and the LD zonal $\dot{Z}$ field, indicating (as do the $\dot{\phi}_{ni}$ values in Table 2) that the drifts creating LD are mainly westward.

Table 6

R.M.S. INTENSITIES OF VARIOUS COMPONENTS OF 1965 LME SECULAR VARIATION, RELATIVE TO R.M.S. SECULAR VARIATION INTENSITY

n	SV	ND	D	MD	LD
1	100	89	46	5	45
2	100	43	90	50	59
3	100	25	92	50	92
4	100	3	100	40	81
5	100	29	87	87	63
6	100	0	100	75	56

Table 6 shows, for the 1965 LME data, the r.m.s. intensities of the various components of each order SV field relative to the r.m.s. SV intensities. The dipole is unique as the only field where the ND component dominates the D component, which is almost purely LD. The westward drift is apparent again since the fifth- and sixth-order fields are the only fields where MD dominates LD. However, it is noted that, owing to the amplification of the fifth- and sixth-order fields associated with inward extrapolation of the field, the previous sentence implies that the MD field plays a major part in determining the geometry of the total field at the core–mantle interface.

Figures 2(*a*)–2(*e*) are isoline maps at the Earth's surface of the rate of change of vertical intensity, $\dot{Z}$, for the fields SV, ND, D, LD, and MD respectively. The spacing of the contour lines in Figure 2(*b*) depicts a relatively flat ND field, signifying slowly changing surface gradients, or small values for the horizontal components $\dot{X}$ and $\dot{Y}$ of ND. There is a high correlation between the isoporic foci in map 2(*b*) and those of the main field quadrupole (a map of which can be found in Winch and Slaucitajs 1966*b*) although the overall structure of ND is not quadrupolar. As Table 5 shows, this high correlation is due to the dominating second-order coefficients $\dot{g}_2^m(ND)$ and $\dot{h}_2^m(ND)$ ($m = 0,1,2$), which according to equation (9) are proportional to the main field quadrupole coefficients. The main difference arises from the large $\dot{g}_1^0(ND)$ coefficient which, weighting the harmonic $\mathrm{P}_1^0(\cos\theta) = \cos\theta$, is probably responsible for the one dipole-like *ND* zero line. A comparison of maps 2(*a*) and 2(*b*) shows that the Antarctic *SV* anomaly is the only large anomaly preserved in *ND* although its magnitude is reduced by about 50%. The very steep gradients, indicating large horizontal components, of the *SV* Atlantic Ocean focus in map 2(*a*) are also greatly diminished in the *ND* field. In contrast map 2(*c*) shows that *D* preserves in general detail the shape of the *SV* field, although there has been an increase in $\dot{Z}$ near the north pole and a decrease near the south pole. This is in accord with the conclusion drawn from Table 6 that *D* generally dominates *ND*. A quick impression gained from maps 2(*d*) and 2(*e*) is that *LD* consists basically of four cells of the $n = m = 2$ type whereas *MD* consists of three cells of the $n = 2$, $m = 0$ type. These shapes are due to the dominating coefficients $\dot{h}_2^2(LD)$ and $\dot{g}_2^0(MD)$ (see Table 5). A particularly interesting result derived from the maps is the conclusion that the large Atlantic *SV* focus is almost entirely caused by the *LD* field.

Table 7

COMPARISON OF R.M.S. VERTICAL INTENSITIES USING 1965 LME DATA

Units are $\gamma\,\mathrm{yr}^{-1}$

Region	*SV*	*ND*	*D*	*LD*	*MD*
World	57	27	49	36	27
Canada	16	16	30	12	21
Australia	15	7	13	6	7

Whitham (1958) has examined *SV* in Canada and interpreted its relatively small magnitude by showing, with methods similar to those used for deriving equation (3), that the best-fit westward drift based on Canadian data was very small and that only a slightly larger meridional drifting effect was present. Table 7 shows the r.m.s. $\dot{Z}$ intensities for the various *SV* components over the world, Canada ($15^\circ \leqslant \theta \leqslant 45^\circ$, $210^\circ \leqslant \phi \leqslant 310^\circ$), and, for comparison, a region ($105^\circ \leqslant \theta \leqslant 135^\circ, 105^\circ \leqslant \phi \leqslant 165^\circ$) that includes most of Australia. It is seen that in Canada *MD* does dominate *LD*, both being significantly smaller than the world values, but that *D* is still larger than *ND*. (Strictly speaking these results, based on world charts, may not be directly comparable with Whitham's which were based on Canadian charts.) The Australian region was chosen for comparison with Canada since Figures 2(*a*)–2(*e*) show that the components of *SV* are small in this region also; the zero lines of $\dot{Z}$ pass close to the continent and, even allowing for some Mercator distortion, the contours are relatively flat indicating small horizontal components. Table 7 indicates that *SV* in Australia is about the same magnitude as in Canada but all the components of *SV* (namely *ND*, *D*, *LD*, and *MD*) are less than half the Canadian values. The *LD* field is particularly small, being about one-sixth of the world r.m.s. value. To the author's knowledge there is no investigation, like Whitham's for Canada, of westward drift effects in Australia, but the small effect predicted by Table 7 is given some support by the secular variation work of van der Linden (1966), who found that the net change in declination in Australia between 1912 and 1962 was associated with only a small westward drift of the declination isolines.

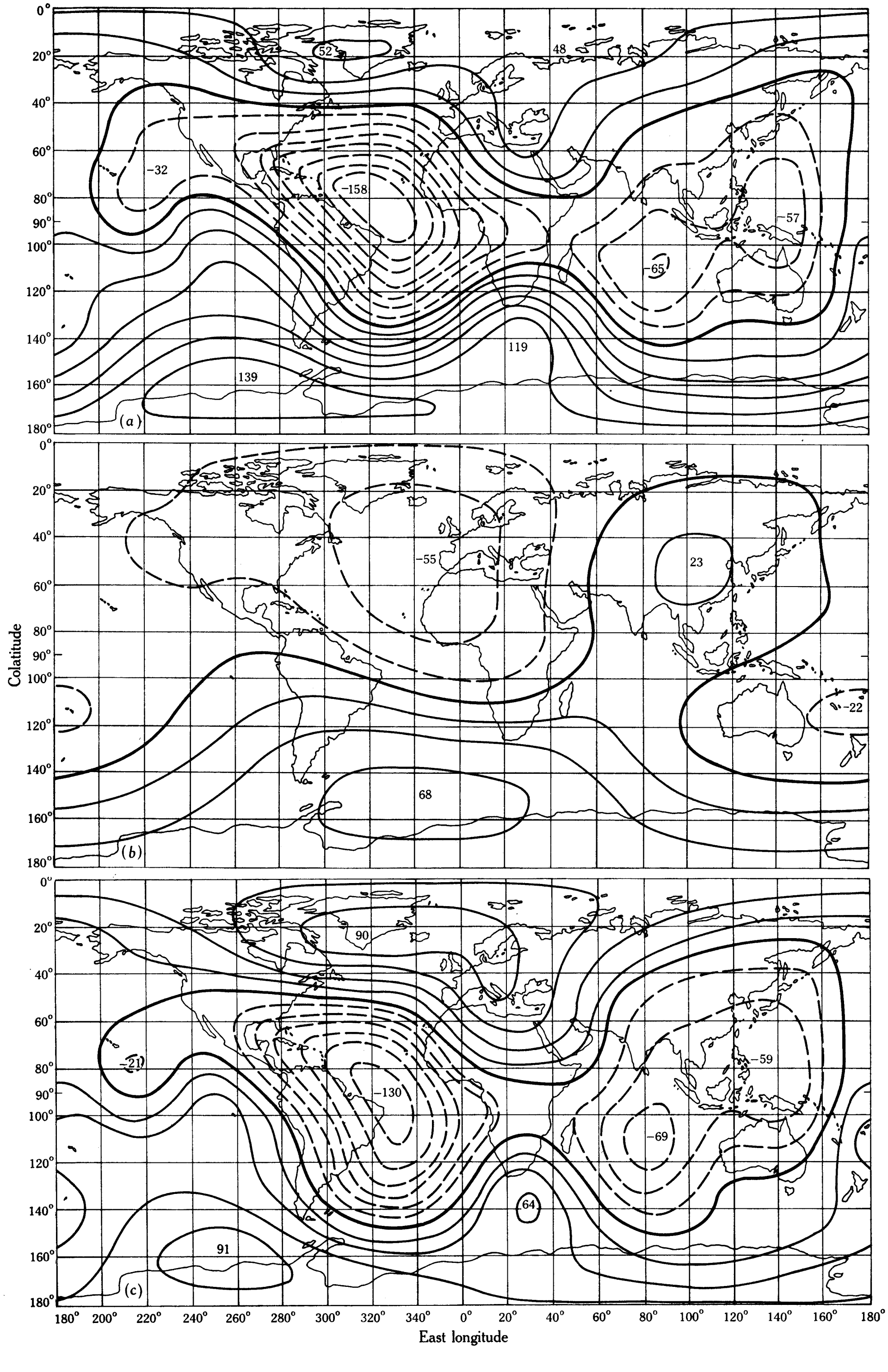
(a)
52
48
-32
-158
-57
-65
119
139
(b)
-55
23
-22
68
(c)
90
-21
-130
-59
-69
64
91
Colatitude
East longitude
0°
20°
40°
60°
80°
90°
100°
120°
140°
160°
180°
180° 200° 220° 240° 260° 280° 300° 320° 340° 0° 20° 40° 60° 80° 100° 120° 140° 160° 180°

It would be interesting to compare the separation of SV in this paper with a separation based on fluid velocities found from a magnetohydrodynamical model of the Earth's outer core (Kahle, Ball, and Vestine 1967; Kahle, Vestine, and Ball 1967; Vestine, Ball, and Kahle 1967). This will be done when fluid velocity data become available in suitable form.

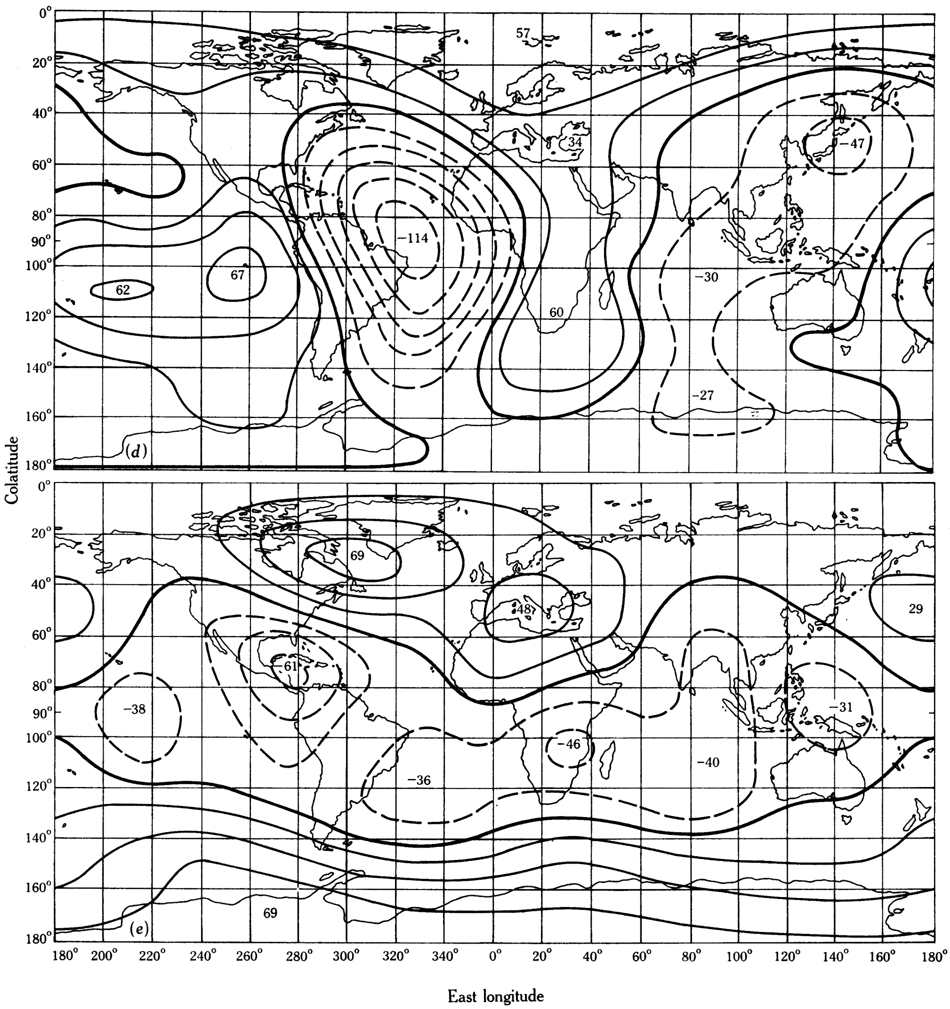

Figs 2(a)–2(e).—Vertical intensity isolines on the Earth's surface (with a contour interval of 20 $\gamma\,\mathrm{yr}^{-1}$) for the 1965 LME geomagnetic secular variation and its components:

(a) secular variation (SV),

(b) non-drifting component (ND),

(c) drifting component (D),

(d) longitudinal drifting component (LD),

(e) meridional drifting component (MD).

Conclusions

Multipole strength has been shown to be a reliable indicator of field intensity, being approximately proportional to the r.m.s. intensity. Non-dipole field strengths have generally increased between 1845 and 1965 but the continued decrease in dipole strength has led to an overall loss of the Earth's magnetostatic energy in space at a rate of about 0·08% per year. However, the geomagnetic secular variation is principally due to drifting rather than decay or growth; longitudinal drifting effects generally dominate meridional drifting effects (in particular, the large Atlantic Ocean anomaly is a longitudinal drifting effect) although the reverse may be true at the core–mantle boundary. The longitudinal drifting is mainly westward so that the overall field has westward drifting characteristics, but it is emphasized that the westward drift is not uniform and on occasions is dominated by meridional drifts and non-drifting contributions. The various components of SV are especially small over Canada (in agreement with Whitham 1958) but less than half as small again over a region of similar area which includes most of Australia.

References

Bullard, E. C. (1953).—*J. geophys. Res.* **58,** 277.

Bullard, E. C., Freedman, C., Gellman, H., and Nixon, J. (1950).—*Phil. Trans. R. Soc.* A **243,** 67.

Cain, J. C., and Langel, R. A. (1968).—Magnetic Survey of the Earth by the OGO–2 and 4 Spacecraft. Paper read at 1968 Washington meeting of Int. Assoc. Geomag. Aeron.

Fanselau, V. G., Kautzleben, H., Lucke, O., Mauersberger, P., and Sellien, K. (1964).—*Geofis. pura appl.* **57,** 5.

Fougere, P. F. (1965).—*J. geophys. Res.* **70,** 2171.

James, R. W. (1968).—*J. Geomagn. Geoelect., Kyoto* **20,** 429.

James, R. W. (1969).—*Geophys. J. R. astr. Soc.* **17,** 305.

Kahle, A. B., Ball, R. H., and Vestine, E. H. (1967).—*J. geophys. Res.* **72,** 4917.

Kahle, A. B., Vestine, E. H., and Ball, R. H. (1967).—*J. geophys. Res.* **72,** 1095.

Leaton, B. R., and Malin, S. R. C. (1967).—*Nature, Lond.* **213,** 1110.

Leaton, B. R., Malin, S. R. C., and Evans, M. J. (1965).—*J. Geomagn. Geoelect., Kyoto* **17,** 186.

van der Linden, J. (1966).—Secular variation of the magnetic field, Australia, 1915–1965. Aust. Dept National Development, Bureau Mineral Resources Record No. 1966/87.

McDonald, K. L., and Gunst, R. H. (1967).—An analysis of the Earth's magnetic field from 1835 to 1965. U.S. Dept Commerce ESSA Tech. Rep. IER 46–IES 1.

Macht, H. G. (1954).—*J. geophys. Res.* **59,** 369.

Maxwell, J. C. (1892).—"Treatise on Electricity and Magnetism." 3rd Ed. Vol. 1, Ch. 9. (Oxford Univ. Press.)

Nagata, T. (1962).—Proc. Benedum Earth Magnetism Symp. p. 39. (Pittsburgh Univ. Press.)

Nagata, T. (1965).—*J. Geomagn. Geoelect., Kyoto* **17,** 263.

Vestine, E. H., Ball, R. H., and Kahle, A. B. (1967).—*J. geophys. Res.* **72,** 4927.

Vestine, E. H., Sibley, W. L., Kern, J. W., and Carlstedt, J. L. (1963).—*J. Geomagn. Geoelect., Kyoto* **15,** 47.

Whitham, K. (1958).—*Can. J. Phys.* **36,** 1372.

Winch, D. E. (1967*a*).—*Geofis. pura appl.* **67,** 112.

Winch, D. E. (1967*b*).—*Geofis. pura appl.* **68,** 90.

Winch, D. E. (1968).—*J. Geomagn. Geoelect., Kyoto* **20,** 205.

Winch, D. E., and Slaucitajs, L. (1966*a*).—*Geofis. pura appl.* **63,** 121.

Winch, D. E., and Slaucitajs, L. (1966*b*).—*Geofis. pura appl.* **65,** 95.

Yukutake, T. (1962).—*Bull. Earthq. Res. Inst. Tokyo Univ.* **40,** 1.

Zolotov, I. G. (1966).—*Geomag. Aeron.* **6,** 413.

Appendix

The method of calculating the derivatives $\dot{M}_n$ and $\dot{\boldsymbol{u}}_{ni}$ $(i = 1, \ldots, n)$ is outlined here in a more general context. Suppose it is required to find the values of k variables x_i $(i = 1, \ldots, k)$ and their derivatives $\dot{x}_i$, given the k nonlinear equations

$$f_i(x_1, \ldots, x_k) = a_i\,, \qquad i = 1, \ldots, k\,, \tag{A1}$$

based on the data a_i with known derivatives $\dot{a}_i$.

The differential form of (A1) is, in vector notation,

$$\mathbf{J}\,\mathrm{d}\boldsymbol{x} = \mathrm{d}\boldsymbol{a}\,, \tag{A2}$$

where $\mathbf{J}$ is the Jacobian matrix with ijth element $\partial f_i/\partial x_j$. Thus, with Greek indices indicating stages of iteration, the Newton–Raphson scheme for solving (A1) is

$$\boldsymbol{x}^{\alpha+1} = \boldsymbol{x}^{\alpha} + \Delta\boldsymbol{x}^{\alpha}\,,$$

where $\Delta\boldsymbol{x}^{\alpha}$ is the solution of

$$\mathbf{J}^{\alpha}\,\Delta\boldsymbol{x}^{\alpha} = \Delta\boldsymbol{a}^{\alpha}\,. \tag{A3}$$

Here $\Delta\boldsymbol{a}^{\alpha} = \boldsymbol{a} - \boldsymbol{f}(x_1^{\alpha}, \ldots, x_k^{\alpha})$, and $\mathbf{J}^{\alpha}$ is matrix $\mathbf{J}$ evaluated using the α-stage iterate $\boldsymbol{x}^{\alpha}$. Required accuracy for $\boldsymbol{x}$ is obtained at some stage $\alpha = \beta$, say, when $\Delta\boldsymbol{x}^{\alpha}$ and $\Delta\boldsymbol{a}^{\alpha}$ in (A3) are sufficiently small.

From (A2) the time derivative $\dot{\boldsymbol{x}}$ satisfies the equation $\mathbf{J}\dot{\boldsymbol{x}} = \dot{\boldsymbol{a}}$, or, to sufficient accuracy, $\mathbf{J}^{\beta}\,\dot{\boldsymbol{x}} = \dot{\boldsymbol{a}}$. However, matrix $\mathbf{J}^{\beta}$ has already been inverted in the β-stage iteration loop to find $\Delta\boldsymbol{x}^{\beta}$. Thus the derivatives $\dot{M}_n$ and $\dot{\boldsymbol{u}}_{ni}$ $(i = 1, \ldots, n)$ are found as a simple by-product of the Newton–Raphson iteration technique employed in the method of multipole analysis outlined in Part I.